Chinese Chemical Letters 34 (2023) 107943

Contents lists available at ScienceDirect

Chinese Chemical Letters

journal homepage: www.elsevier.com/locate/cclet

Core-shell lipid-polymeric nanoparticles for enhanced oral bioavailability and antihypertensive efficacy of KY5 peptide

Jingmei Yuan[a,1], Mengran Guo[a,1], Shengnan Zhao[b], Jinhua Li[a], Xinchun Wang[c], Jian Yang[b,*], Zhaohui Jin[a,*], Xiangrong Song[a,c,*]

[a] Department of Critical Care Medicine, Department of Clinical Pharmacy, Frontiers Science Center for Disease-related Molecular Network, State Key Laboratory of Biotherapy and Cancer Center, West China Hospital, Sichuan University, Chengdu 610041, China
[b] School of Applied Chemistry and Biological Technology, Shenzhen Polytechnic, Shenzhen 518055, China
[c] First Affiliated Hospital of the Medical College, Shihezi University, Shihezi 832008, China

ARTICLE INFO

Article history:
Received 21 June 2022
Revised 22 October 2022
Accepted 24 October 2022
Available online 27 October 2022

Keywords:
Hypertension
Core-shell lipid-polymeric nanoparticles
KY5
Antihypertensive peptides
Oral delivery

ABSTRACT

Hypertension is the leading risk factor for death and disability, and hypertensive patients always need long-term oral antihypertensive drugs. Some bioactive peptides that extracted from animals or plants have shown excellent advantages on antihypertension. However, the oral delivery of these peptides is always failure on account of instability and poor absorption in the gastrointestinal tract. Herein, we developed a core-shell lipid-polymeric nanoparticle for oral delivery of a highly efficient antihypertensive peptide KY5 (KY5-CSs). KY5-CSs had a particle size of 216.7 ± 2.5 nm, with a narrow PDI of 0.07 ± 0.01. The zeta potential was −4.1 ± 0.1 mV. It exhibited good stability in 4 °C and possessed a controlled release behavior in gastrointestinal tract. The cellular uptake study proved that the lipid shell imparted unique capability of permeation across the mucus layer and internalization by Caco-2/HT-29 cells. In addition, KY5-CSs enhanced *in situ* intestinal absorption in SD rats. The pharmacokinetic studies and antihypertensive efficacy showed a superior oral absorption and antihypertensive effect of KY5-CSs than KY5-NPs. In conclusion, the core-shell lipid-polymeric nanoparticles will provide attractive potential for oral delivery of antihypertensive peptides.

© 2023 Published by Elsevier B.V. on behalf of Chinese Chemical Society and Institute of Materia Medica, Chinese Academy of Medical Sciences.

Hypertension is a growing burden emerging as one of the major healthcare challenges worldwide [1]. The International Society of Hypertension has defined a blood pressure (BP) reading of over 140/90 mmHg as hypertensive. It is recommended that pharmacological treatment is applied if lifestyle interventions fail to manage high BP [2]. Commercial antihypertensive drugs, such as angiotensin converting enzyme (ACE) inhibitors, angiotensin receptor blockers, calcium channel blockers, β-blockers, and diuretics, exhibit positive BP-lowering effects alone or in combination therapy. However, these synthetic drugs always have side effects, such as taste disturbances, tussis, headache, erythra and dizziness [3–5]. Over the past two decades, many antihypertensive peptides that inhibit ACE have been isolated from food, plants, and animals. These peptides are usually more efficient and safer than synthetic drugs on the market [6,7], and they exhibit excellent development potential [8] due to their excellent biocompatibility and biodegradability [9]. However, most peptides are fragile and easily degraded in the gastrointestinal tract (GIT) before they reach the absorption position. Furthermore, the mucus layer, tight junctions and intestinal epithelial cells provide a physical barrier to limit the oral uptake of macromolecules such as peptides [10,11]. These obstacles hinder the application of antihypertensive peptides.

To solve these problems, polymer-based controlled drug delivery systems have been developed, such as poly-lactic acid (PLA), poly-ε-caprolactone, chitosan, and poly-γ-glutamic acid (PGA) [12–15]. Recently, Han *et al.* developed a DSPE-PCB (poly-carboxybetaine conjugated to 1,2-distearoyl-*sn*-glycero-3-phosphoethanolamine) micelle for the oral delivery of insulin, which showed a high oral bioavailability of >40% [16]. Liu and Zhong loaded cyclosporine A with functional chitosan nanoparticles, which increased its oral bioavailability three times [17]. To increase the stability of liraglutide in the GIT, Uhl *et al.* designed a surface-modified PLA nanoparticle to load liraglutide, and the oral bioavailability of liraglutide increased by 4.5 times [18]. Poly(lactic-*co*-glycolic acid) (PLGA) has been widely used for peptide delivery. It exhibited good biocompatibility and was approved by the Food and Drug Administration (FDA) [19–21]. PLGA can encapsu-

* Corresponding authors.
E-mail addresses: jiany@szpt.edu.cn (J. Yang), 695025422@qq.com (Z. Jin), songxr@scu.edu.cn (X. Song).
[1] The authors contributed equally to this work.

https://doi.org/10.1016/j.cclet.2022.107943
1001-8417/© 2023 Published by Elsevier B.V. on behalf of Chinese Chemical Society and Institute of Materia Medica, Chinese Academy of Medical Sciences.

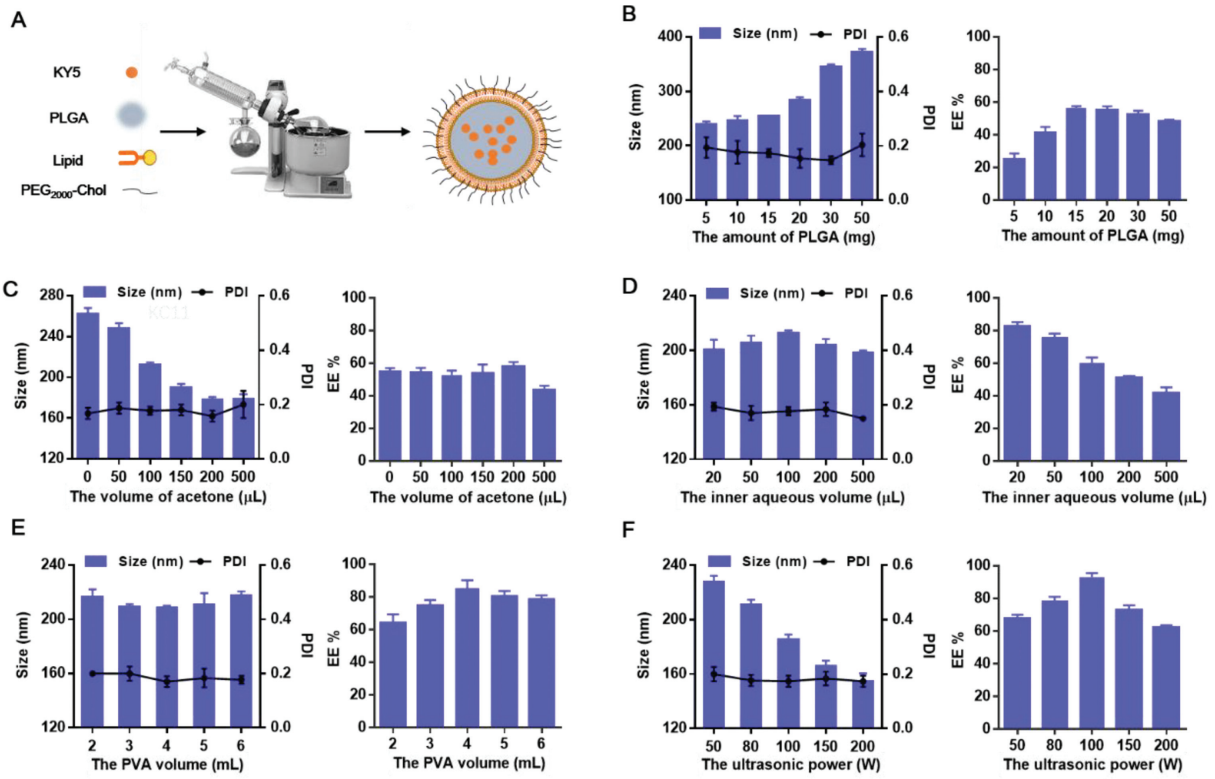

Fig. 1. Schematic illustration of the preparation of KY5-CSs (A) and the effect of prescription and processing parameters such as (B) the amount of PLGA, (C) the volume of acetone, (D) the inner aqueous volume, (E) the volume of PVA, and (F) the ultrasonic power on the particle size and encapsulation efficiency of KY5-CSs.

late peptides and effectively protect them from degradation in the GIT. In addition, the controllable release behavior of peptides from PLGA nanoparticles can maintain the blood concentration and pesticide effect [22–24]. For antihypertensive peptide delivery, PLGA is popular for encapsulating peptides. Castro *et al.* have developed a PLGA nanoparticle with mucoadhesive guar-gum films for buccal delivery of antihypertensive peptide [23]. The combination system showed higher permeation ability in the TR146 cell multilayer. Yu *et al.* encapsulated VP5 into PLGA nanoparticles (PLGANPs) [25]. The PLGANPs enhanced the oral bioavailability and antihypertensive efficacy of VP5. Nevertheless, PLGA nanoparticles still face some problems for the oral delivery of bioactive peptides, such as (i) the surface of PLGA nanoparticles is hydrophobic, which is limited to interacting with the mucosal surface, resulting in easy removal under peristalsis, (ii) the permeation of PLGA nanoparticles containing bioactive peptides through the mucus layer is not efficient [25,26], and (iii) PLGA nanoparticles are too rigid that internalization through enterocytes is limited [27,28]. Therefore, it is necessary to increase the surface hydrophilicity and reduce the rigidity of PLGA nanoparticles. A phospholipid bilayer, such as liposomes, is a self-assembled system consisting of phospholipid molecules and cholesterol. The hydrophilic surface, high biocompatibility and deformability of liposomes make them promising peptide vehicles for oral delivery. However, simple liposomes are instable in the GIT, and peptides are prone to leakage. To overcome these disadvantages of the two nanocarriers, a lipid-polymeric nanoparticle may be available due to the high encapsulation efficiency of PLGA and the biocompatibility and fluidity of phospholipids [29,30]. This core nanoparticle supported lipid membrane nanocarrier is supposed to enhance the oral bioavailability and prolong the circulation time [31]. Moreover, the nontoxic components and simple preparation process make it competitive in clinical translation [32]. Nevertheless, whether lipid-polymeric nanoparticles facilitate mucus penetration and intestinal absorption of peptides is not fully understood.

Lys-Tyr-Leu-Cys-Tyr (KYLCY, KY5) is an ACE inhibitory peptide with an excellent antihypertensive effect. To improve the oral bioavailability and antihypertensive effect of KY5, we designed a core-shell lipid-polymeric nanoplatform (KY5-CSs) to load KY5. The formulation parameters of KY5-CSs were systematically investigated, and the physicochemical properties, including particle sizes, zeta potentials, morphologies, and stabilities, were comprehensively assessed. Additionally, an *in vitro* release study, cellular uptake and *in situ* absorption study were implemented. Finally, pharmacokinetics and pharmacodynamics studies were conducted to evaluate the antihypertensive effect. The materials and experimental procedure are described in Supporting information, and all the animal experiments were approved by the Animal experimental ethics committee of State Key Laboratory of Biotherapy of Sichuan University.

In this study, KY5-CSs were prepared using a modified thin-film hydration-homogeneous dispersion method (Fig. 1A). The optimization of KY5-CSs was performed from the prescription and preparation processes using a single factor analysis. As shown in Fig. 1B, the particle size and encapsulation efficiency of KY5-CSs increased as the PLGA amount increased. When the amount of PLGA was 15 mg, KY5-CSs had a proper encapsulation efficiency and smallest particle size. The acetone in the organic phase helped to control the particle size but had little effect on the encapsulation efficiency (Fig. 1C). As the volume of acetone reached 200 μL, a higher encapsulation efficiency and smaller particle size were obtained. The inner aqueous volume had a great influence on the encapsulation efficiency of KY5-CSs. From Fig. 1D, the encapsulation efficiency decreased with increasing inner aqueous volume; thus, 20 μL of inner aqueous solution was chosen. In addition, as the volume of PVA increased, a slight upward trend of encapsulation

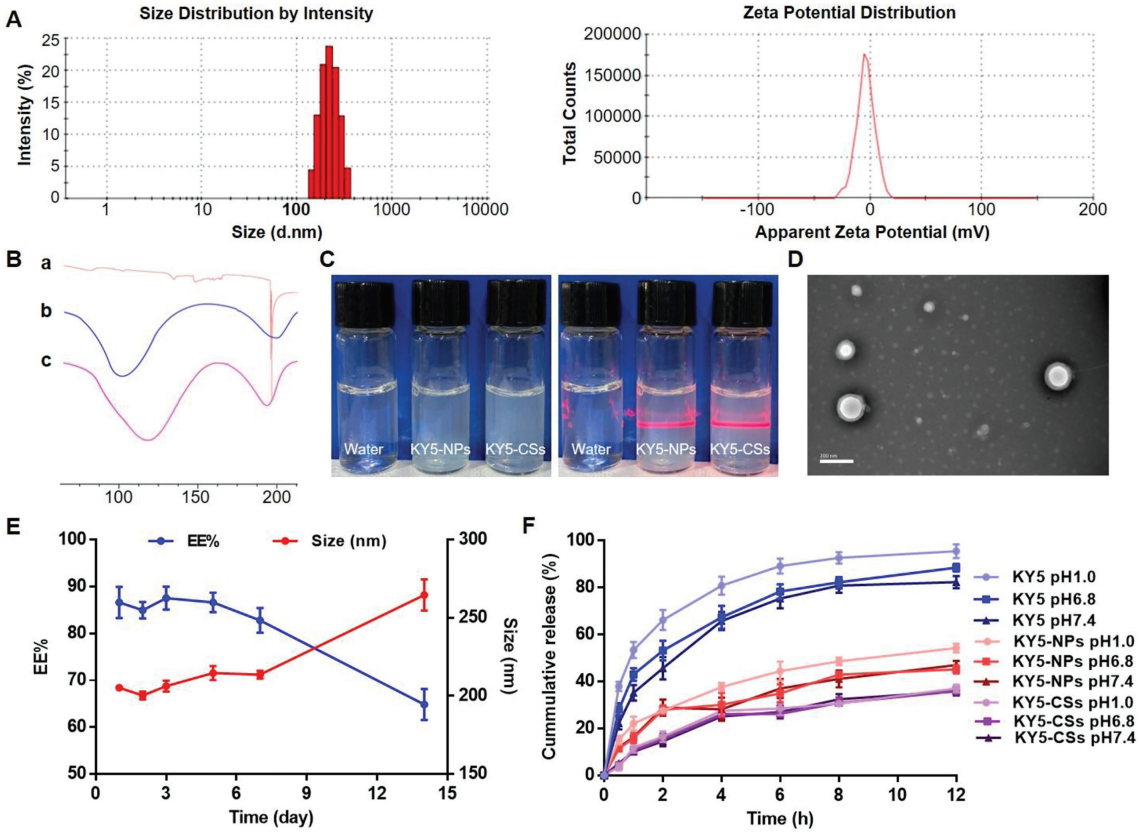

Fig. 2. Physical-chemical properties of KY5-CSs. (A) Size distribution and zeta potential of KY5-CSs. (B) DSC curves of (a) free KY5, (b) KY5-NPs and (c) KY5-CSs. (C) The appearance under sunlight and the Tyndall effect under laser radiation. (D) TEM images of KY5-CSs. (E) Changes in encapsulation efficiency and particle size of KY5-CSs when stored at 4 °C for 14 days. (F) Release profiles of free KY5, KY5-NPs and KY5-CSs in different phosphate buffers (pH 1.2, 6.8, and 7.4).

efficiency and a fluctuation of particle size were observed (Fig. 1E). As the ultrasound power increased from 50 W to 200 W, the particle size decreased constantly, while the ultrasound power exhibited the best encapsulation efficiency when the power was 100 W (Fig. 1F). In addition, there was no significant change in PDI in all groups. The optimal KY5-CSs were used for the following studies.

The particle size and PDI of the optimal KY5-CSs were measured using a dynamic light scattering method. As shown in Fig. 2A, the average particle size of KY5-CSs was 216.7 ± 2.5 nm with a narrow size distribution (PDI = 0.07 ± 0.01). The zeta potential was −4.1 ± 0.1 mV. In addition, the encapsulation efficiency of KY5-CSs was 89.88% ± 1.23%, and the drug loading was 1.54% ± 0.25%. The DSC pattern (Fig. 2B) showed that free KY5 presented an endothermic peak at 195.8 °C followed by an exothermic peak, probably due to its degradation. For KY5-NPs and KY5-CSs, the endothermic peak of KY5 disappeared, while the two broadening endothermic peaks at 125.2 °C and 195.6 °C corresponded to the glass transition temperature (T_g) of PLGA and PVA, respectively. This suggested that KY5 in KY5-NPs and KY5-CSs were in an amorphous or molecular state. The appearance of the preparations is shown in Fig. 2C. The colloidal solution exhibited slight blue opalescence under sunlight and a strong Tyndall effect under laser radiation. The TEM images (Fig. 2D) showed that KY5-CSs were generally spherical and homogeneous with a core-shell structure. The particle diameters ranged from 170 nm to 240 nm, which was in good agreement with the narrow particle size distribution.

In the stability study, KY5-CSs displayed good stability with no detectable changes in particle sizes and encapsulation efficiency for at least 5 days (Fig. 2E). When KY5-CSs were stored beyond 5 days, an enlargement of particle size and a reduction in encapsulation efficiency were detected. Thus, KY5-CSs were suggested to be stable at 4 °C for five days. It could be further investigated to develop a freeze-drying formulation for long-term storage.

The *in vitro* release profiles of KY5 from KY5-CSs are presented in Fig. 2F. Free KY5 showed an obvious burst release behavior in all release media. After 8 h, 100% of the free KY5 was released. When loaded in KY5-NPs, only approximately 30% of KY5 was released from KY5-NPs in all the release media. In addition, approximately 20% of the KY5 was released from the KY-CSs. The results suggested that KY5-NPs and KY5-CSs exhibit controlled release behavior. In addition, KY5-CSs could better protect against KY5 than KY5-NPs due to the existence of lipid membranes.

To explore the penetration efficiency of Cou-6-NPs and Cou-6-CSs in the small intestinal mucus layer, porcine mucus was spread in a Transwell membrane. As shown in Fig. 3A, Cou-6-CSs showed significant ($P < 0.001$) improvement in transport from the upper side of the mucus to the lower side. This may be due to PEG_{2000}, and the phospholipid bilayer on the surface of Cou-6-CSs increased the hydrophilicity of the particles, which facilitated penetration [33–35].

After penetrating through the mucus layer, the KY5-CSs were supposed to be absorbed from intestinal epithelial cells before entering the systemic circulation. Herein, the cellular uptake of the preparations was investigated in Caco-2/HT-29 coculture cells. The FCM results (Fig. 3B) showed that the uptake of free Cou-6, Cou-6-NPs and Cou-6-CSs was time-dependent in Caco-2/HT-29 cells. The mean fluorescence intensities (MFIs) of the three preparations achieved a balance after 2 h of incubation. The MFI of Cou-6 was the lowest because free Cou-6 in Caco-2/HT-29 cells was absorbed through passive diffusion [36]. Cou-6-NPs can enhance cellular uptake by endocytosis [37,38]. The MFI of Cou-6-CSs was the highest from 0.5 h to 2 h in Caco-2/HT-29 cells. This may result from the

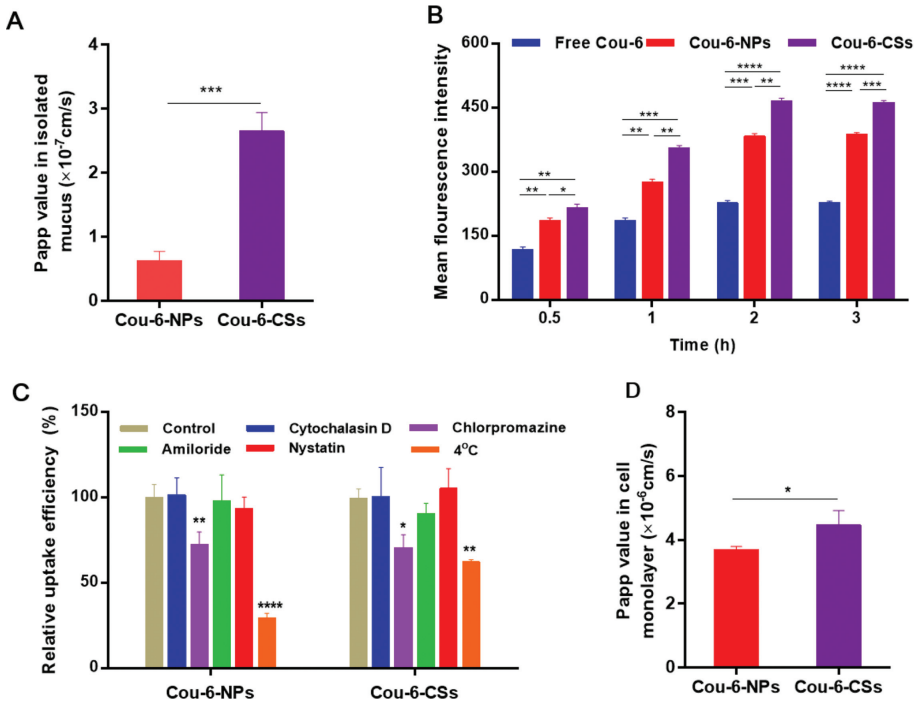

Fig. 3. (A) Papp values of Cou-6-NPs and Cou-6-CSs across the mucus. (B) The MFIs of Caco-2/HT-29 cells treated with free Cou-6, Cou-6-NPs and Cou-6-CSs for 3 h. (C) Endocytosis mechanisms of Cou-6-NPs and Cou-6-CSs on Caco-2/HT-29 cells. (D) Papp value of Cou-6-NPs and Cou-6-CSs transported across Caco-2/HT-29 monolayers. Data are the mean ± SD ($n = 3$). $^{*}P < 0.05$, $^{**}P < 0.01$, $^{***}P < 0.001$ and $^{****}P < 0.0001$ *vs.* control.

good biocompatibility and viscoelasticity of the phospholipid shell. Additionally, the MFI of Cou-6-CSs in Caco-2/HT-29 cells was 2.11 and 1.24 times higher than those of free Cou-6 and Cou-6-NPs after 2 h of incubation.

To identify the endocytosis pathways of Cou-6-NPs and Cou-6-CSs, the endocytosis mechanism was further investigated in Caco-2/HT-29 cells using uptake inhibitors, including chlorpromazine, nystatin, amiloride and cytochalasin D. These inhibitors were used to inhibit clathrin-mediated endocytosis, caveolin-mediated endocytosis, macropinocytosis and phagocytosis [39–41], respectively. The uptake of Cou-6-NPs and Cou-6-CSs by Caco-2/HT-29 cells without endocytosis inhibitors was defined as the control group. As shown in Fig. 3C, both Cou-6-NPs and Cou-6-CSs showed significantly reduced cellular uptake at 4 °C. Low temperature is known to suppress the production of adenosine triphosphate (ATP) in cells, thus hindering endocytic pathways [42]. The internalization of Cou-6-NPs and Cou-6-CSs was energy dependent. In addition, chlorpromazine significantly decreased the uptake rate of Cou-6-NPs and Cou-6-CSs by Caco-2/HT-29 cells, indicating that clathrin-mediated endocytosis was involved in their cellular uptake.

To better mimic mucosal tissues, Caco-2/HT-29 cocultured cell monolayers were used to investigate the effect of lipid shell modification on the transcytosis of KY5-NPs [43,44]. Then, the Papp values were calculated to evaluate the transepithelial transport rate of KY5-NPs and KY5-CSs. As shown in Fig. 3D, the Papp value of Cou-6-CSs was 1.4-fold higher than that of Cou-6-NPs. This resulted from the good compatibility of the lipid shell with the cell membrane, which enhanced the endocytosis and exocytosis of NPs [30]. Moreover, Cou-6-CSs have a semielastic structure, which is conducive to cellular uptake [45].

To further assess whether the compatibility of KY5-NPs with intestinal epithelium *in vivo* would be improved after lipid shell modification, *in situ* intestinal loop models were constructed using SD rats. Cou-6-NPs and Cou-6-CSs were separately administered into the intestinal loops of the ileum. From the results (Fig. S1 in Supporting information), Cou-6-CSs more easily adhered to the surface of the intestinal villi and entered the inner matrix of the villi. The results revealed that the phospholipid bilayer facilitated the adhesion of nanoparticles to the mucus and internalization into the intestinal epithelium.

To study the *in vivo* behavior of the formulations, Cou-6-NPs and Cou-6-CSs were administered by oral gavage (Fig. 4A), and the blood concentration of Cou-6 was measured. The pharmacokinetic profiles are shown in Fig. 4B, and the pharmacokinetic parameters are listed in Table S1 (Supporting information). After oral administration, Cou-6-CSs exhibited faster and higher absorption than Cou-6-NPs. The area under the curve ($AUC_{0\text{-}24\ h}$) was 3.2-fold that of Cou-6-NPs. In addition, the maximum concentration (C_{max}) of Cou-6-CSs was 4.0 times higher than that of Cou-6-NPs. These results demonstrated that Cou-6-NPs modified with a phospholipid bilayer could significantly improve the bioavailability of bioactive peptides.

In the antihypertensive efficacy study, SHRs were randomly divided into four groups (control, free KY5, KY5-NPs, and KY5-CSs) to measure the blood pressure lowering effect of the formulations. In Fig. 4C, free KY5, KY5-NPs and KY5-CSs all had significant effects on lowering blood pressure. While free KY5 can only reduce blood pressure to 196 mmHg for 9 h, KY5-NPs and KY5-CSs showed enhanced and lasting antihypertensive effects compared with free KY5. At 96 h post-administration, the systolic blood pressure (SBP) of KY5-NPs increased to the initial level, while the antihypertensive effect lasted for 144 h of KY5-CSs. In addition, KY5-CSs showed the best blood pressure lowering effect at 9 h post-treatment, with blood pressure reducing to 172 mmHg. These results suggested that KY5-NPs and KY5-CSs could protect against and slowly release KY5. KY5-CSs exhibited superior long-term antihypertensive efficacy.

In this study, we designed a core-shell lipid-polymeric nanoparticle platform (KY5-CSs) to deliver a water-soluble KY5 peptide for hypertension therapy. KY5-CSs were successfully prepared by a modified thin-film hydration-homogeneous dispersion method with high encapsulation efficiency. The phospholipid bilayer covering the surface of the nanoparticles enhanced mucus penetration,

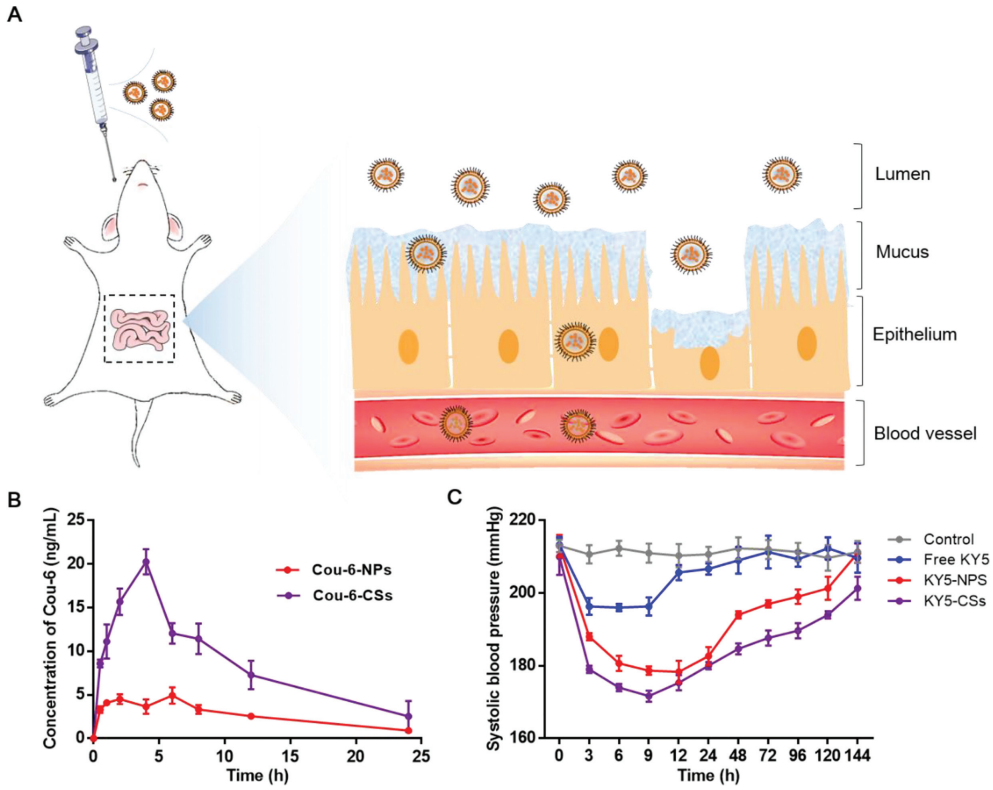

Fig. 4. (A) Schematic illustration of the process of KY5-CSs penetration across mucus and epithelial barriers. (B) Plasma concentration *versus* time profiles of Cou-6 after oral administration of Cou-6-NPs and Cou-6-CSs at a dosage of 1 mg/kg ($n = 4$). (C) Changes in SBP after oral administration of free KY5, KY5-NPs and KY5-CSs. Saline was used as a control ($n = 6$).

cellular uptake, transmembrane transport ability and *in situ* internalization for oral antihypertensive peptides. Furthermore, KY5-CSs significantly improved the oral bioavailability and the long-term antihypertensive effect of KY5. In conclusion, the core-shell lipid-polymeric nanoparticles developed in this study have simple preparation technology and good antihypertensive effects. Further evaluation of the safety is considered to facilitate the application of this nanocarrier for oral peptides. Our study provides a promising platform for oral peptide delivery.

Declaration of competing interest

We wish to confirm that there are no known conflicts of interest associated with this publication and there has been no significant financial support for this work that could have influenced its outcome.

Acknowledgments

This study was supported by the Youth Fund of National Natural Science Foundation of China (No. 82104081), the Science and Technology Project of Shenzhen (No. JCYJ20170413155047512), the 1.3.5 project for disciplines of excellence, West China Hospital, Sichuan University (No. ZYGD18020/ZYJC18006), the Sichuan Province Science and Technology Support Program (No. 2020JDRC0052), and the Science and Technology Project of Xinjiang Production and Construction Corps (No. 2022AB020).

Supplementary materials

Supplementary material associated with this article can be found, in the online version, at doi:10.1016/j.cclet.2022.107943.

References

[1] R.R. Dhungana, Z. Pedisic, M. Dhimal, B. Bista, M. de Courten, Glob. Health Action 15 (2022) 2000092.
[2] P. Nugroho, H. Andrew, K. Kohar, C.A. Noor, A.L. Sutranto, Ann. Med. 54 (2022) 837–845.
[3] L. Xue, X. Wang, Z. Hu, et al., Peptides 99 (2018) 161–168.
[4] Q. Wu, Y. Li, K. Peng, et al., J. Agr. Food. Chem. 67 (2019) 8149–8159.
[5] Y. Zheng, X. Wang, Y. Zhuang, et al., Molecules 24 (2019) 4562.
[6] A. Ganguly, K. Sharma, K. Majumder, Adv. Food. Nutr. Res. 89 (2019) 165–207.
[7] J. Gao, Q. Liu, L. Zhao, et al., J. Agr. Food. Chem. 69 (2021) 146–158.
[8] T. Ji, Y. Li, X. Deng, et al., Nat. Biomed. Eng. 5 (2021) 1099–1109.
[9] Y. Liu, D. Li, J. Ding, X. Chen, Chin. Chem. Lett. 31 (2020) 3001–3014.
[10] D.J. Drucker, Nat. Rev. Drug. Discov. 19 (2020) 277–289.
[11] P. Lundquist, P. Artursson, Adv. Drug. Delivery. Rev. 106 (2016) 256–276.
[12] Q. Zhu, Z. Chen, P.K. Paul, et al., Acta. Pharm. Sin. B 11 (2021) 2416–2448.
[13] S. Haddadzadegan, F. Dorkoosh, A. Bernkop-Schnürch, Adv. Drug. Delivy. Rev. 182 (2022) 114097.
[14] A. des Rieux, V. Fievez, M. Garinot, Y.J. Schneider, V. Préat, J. Control. Release 116 (2006) 1–27.
[15] V.V. Khutoryanskiy, Adv. Drug. Deliv. Rev. 124 (2018) 140–149.
[16] X. Han, Y. Lu, J. Xie, et al., Nat. Nanotechnol. 15 (2020) 605–614.
[17] M. Liu, X. Zhong, Z. Yang, Sci. Rep. 7 (2017) 41322.
[18] P. Uhl, C. Grundmann, M. Sauter, et al., Nanomed-Nanotechnol. 24 (2020) 102132.
[19] J. Sheng, H. He, L. Han, et al., J. Control. Release 233 (2016) 181–190.
[20] K. Wang, Y. Feng, S. Li, et al., J. Biomed. Nanotechnol. 14 (2018) 1806–1815.
[21] J. Xu, Y. Zhang, J. Xu, et al., Biomaterials 216 (2019) 119247.
[22] H. Sun, D. Liu, Y. Li, X. Tang, Y. Cong, Int. J. Nanomed. 9 (2014) 1709–1716.
[23] P.M. Castro, P. Baptista, A.R. Madureira, B. Sarmento, M.E. Pintado, Int. J. Pharmaceut. 547 (2018) 593–601.
[24] S. Kecel-Gündüz, Y. Budama-Kilinc, R.C. Koc, et al., J. Biomol. Struct. Dyn. 36 (2018) 2893–2907.
[25] T. Yu, S. Zhao, Z. Li, et al., Int. J. Mol. Sci. 17 (2016) 1977–1989.
[26] P. Ahlin, J. Kristl, A. Kristl, F. Vrecer, Int. J. Pharmaceut. 239 (2002) 113–120.
[27] M. Yu, L. Xu, F. Tian, et al., Nat. Commun. 9 (2018) 2607.
[28] Y. Zheng, L. Xing, L. Chen, et al., Biomaterials 262 (2020) 120323.
[29] L. Zhang, Q. Feng, J. Wang, et al., ACS Nano 9 (2015) 9912–9921.
[30] S. Krishnamurthy, R. Vaiyapuri, L. Zhang, J.M. Chan, Biomater. Sci. 3 (2015) 923–936.
[31] X. Liu, X. Zhong, C. Li, Chin. Chem. Lett. 32 (2021) 2347–2358.
[32] Chunxiong Zheng, M. Li, Jianxun Ding. BIO Integration 2 (2021) 57–60.

[33] X. Zhu, J. Wu, W. Shan, et al., Adv. Funct. Mater. 26 (2016) 2728–2738.
[34] Y. Zhang, H. Li, Q. Wang, et al., Adv. Funct. Mater. 28 (2018) 1–15.
[35] Q. Xu, L.M. Ensign, N.J. Boylan, et al., ACS Nano 9 (2015) 9217–9227.
[36] F. Ravar, E. Saadat, M. Gholami, et al., J. Control. Release 229 (2016) 10–22.
[37] F. Danhier, E. Ansorena, J.M. Silva, et al., J. Control. Release 161 (2012) 505–522.
[38] S.S. Lee, Y.B. Lee, I.J. Oh, J. Pharm. Investig. 45 (2015) 1–9.
[39] L. Liu, W. Yao, X. Xie, J. Gao, X. Lu, J. Nanobiotechnol. 19 (2021) 235.
[40] R. Mo, X. Jin, N. Li, et al., Biomaterials 32 (2011) 4609–4620.
[41] W. De Haes, G. Van Mol, C. Merlin, et al., Mol. Pharmaceut. 9 (2012) 2942–2949.
[42] J. Cao, X. Xie, A. Lu, et al., Biomaterials 35 (2014) 4517–4524.
[43] A. García-Rodríguez, L. Vila, C. Cortés, A. Hernández, R. Marcos, Food. Chem. Toxicol. 113 (2018) 162–170.
[44] J. Wu, Y. Zheng, M. Liu, et al., ACS. Appl. Mater. Interfaces 10 (2018) 9916–9928.
[45] S. Zhao, J. Li, F. Wang, et al., Chin. Chem. Lett. 31 (2020) 1147–1152.